



PRINCIPAL DESIGN OF METHANE-OXYGEN COMBUSTION CHAMBER WITH SUPERCRITICAL CO₂

Komarov I., Kharlamova D., Vegera A. and Makhmutov B.

Department of Innovative Technologies for High-Tech Industries, National Research University MPEI, Moscow, Russia
E-Mail: daria-rostov@yandex.ru

ABSTRACT

The report presents the results of research at the engineering design of a turbomachine combustion chamber running on supercritical carbon dioxide at an ambient pressure of 300 bar. The research method is a numerical simulation of turbulent-kinetic processes in the Ansys Fluent software package using the reduced methane combustion mechanism. Two key features characterize the combustion of methane in CO₂ diluent. Firstly, combustion occurs with a significantly smaller excess of oxidizing agent than in the combustion chamber of traditional gas turbines. Secondly, the normal flame propagation velocity in CO₂ at ultrahigh pressure is much lower than with N₂ diluent. In order to ensure stable and complete burning of fuel, various ways to increase the real burning rate were reviewed - swirling the mixture of fuel and oxidizer, controlling the distribution of diluent over the volume of the combustion chamber, changing the main structural dimensions of the combustion chamber.

Keywords: allam cycle, methane-oxygen combustor, stable combustion, computer simulation, turbulent-kinetic process, reduced combustion description.

INTRODUCTION

Efficient environmentally friendly power production is an important XXI century target. The main part of electric power is produced by the fossil fuel combustion in Thermal Power Plants (TPP) that operate Rankine, Bryton and Rankine-Bryton cycles. The air-fuel mixture combustion products emit a lot of greenhouse gases which increases their content in the Earth atmosphere. Besides this the combustion zone Nitrogen content leads to the toxic Nitrogen oxides emission production. Emission mitigation down to zero values is hardly accessible in the traditional Power industry [1, 2]. The TPP toxic emission problem may be solved by creation of closed thermodynamic cycles with oxygen fuel combustion, or oxy-fuel power facilities. The oxygen fuel combustion produces water vapor and carbon dioxide which is the specific feature and advantage of these cycles. The carbon dioxide may be separated from vapor by the condensing technology with minimal energy wastes.

As to introduce the Oxy-Fuel Power Facilities (OFPF) it is necessary to solve a range of research and development problems including the production equipment theory for the supercritical carbon dioxide operation and especially the combustor design. The combustor inlet carbon dioxide and supercritical pressure influence the combustion stability which needs an investigation. It is directly related to the cycle thermal efficiency and production of non-condensing gases CO, O₂, H₂, radicals H and OH and other products of incomplete fuel combustion. The working fluid contents and thermodynamic parameters determine specific features of the combustion process. In the OFPF combustor natural gas reacts oxygen in the CO₂ diluent environment at 300 bar pressure which is remarkably different from the traditional combustor conditions where pressure is usually below 30 bar and the diluent is atmospheric nitrogen.

Figure-1 shows the Allam cycle that is now one of the most prospective oxy-fuel power production cycles

in terms of maximal production efficiency and environmental friendliness [3, 4].

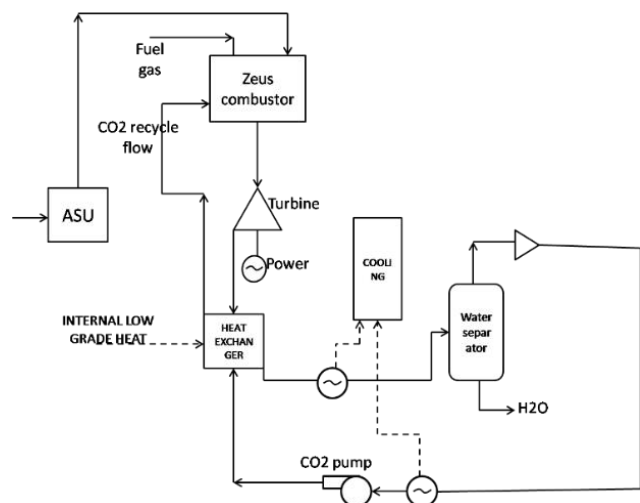


Figure-1. Flow chart of natural gas firing allam cycle.

Published data consider the carbon dioxide content as a chemical reactions inhibitor, at equal conditions and diluent contents the flame propagation velocity in O₂-CO₂ environment is smaller than in the O₂-N₂ mixture one. The CO₂ diluent combustion slowdown effect is caused by the difference of its physical parameters from the N₂ ones. The N₂ also works as a diluent but does not make strong inhibiting effects. The diluents influence difference is due to difference of such parameters as specific heat capacity, heat conductivity, viscosity or diffusion coefficient (ref. Table-1). At similar temperatures the CO₂ specific heat capacity is higher than the N₂ one so at equal flame temperatures combustion in the CO₂ environment requires higher oxidizer content. At similar temperatures the CO₂ and N₂ heat conductivities and viscosities are almost equal but the CO₂ diffusion



coefficient is about 20% lower than the N₂ one which hampers the mixture formation and components diffusion

[5].

Table-1. N₂ and CO₂ heat capacity and diffusion coefficient.

Parameter	N ₂		CO ₂	
Temperature, °C	500	1000	500	1000
Specific heat capacity, c_p , KJ/kg °	1,08	1,20	1,16	1,30
Diffusion coefficient, D , cm ² /s	0,51	1,64	0,39	1,31
Heat transfer coefficient, λ , W/m K	39,0	68,6	33,3	69,1

The pressure influence upon combustion kinetics and flame propagation is ambiguous. Paper [6] shows that higher pressure linearly reduces the flame propagation velocity. Papers [7, 8] write that if the atmospheric pressure flame velocity is below 0.5 m/s at higher pressure the velocity will be higher. The sources of this ambiguous pressure influence upon the combustion velocity is yet not clear.

Paper [9] discloses a set of theoretical investigations with the multi-reaction combustion description GRI-Mesh 3.0 [10] of the OFPF parameters influence and specifically of the diluent mass content γ in the active combustion zone CO₂/(CO₂+O₂) upon the normal flame propagation velocity that is the main reaction parameter.

The investigation determines the main dependencies of physical and chemical processes of CH₄-O₂ mixture oxidation in CO₂ environment. The conclusions are the following:

- CO₂ diluent inhibits chemical reactions. At equal conditions the normal flame propagation velocity in CO₂ diluent environment is 4 times smaller than in the N₂ one (Figure-2).
- At supercritical combustor pressure the normal flame propagation velocity is smaller (Figure-3).
- A 20% reduction of the CO₂ diluent content in active combustion zone increases the normal flame propagation velocity for above 8 times (Figure-4).

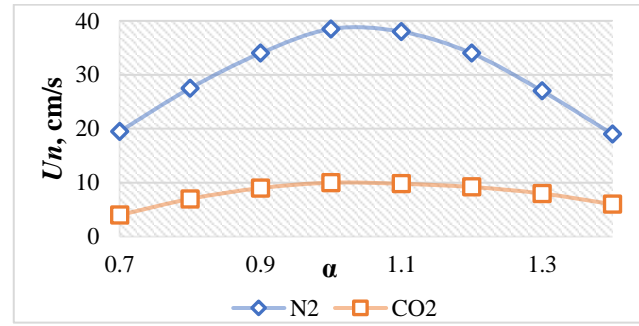


Figure-2. Flame propagation normal velocity in N₂ and CO₂ ($\gamma = 0,79$) diluters environment at atmospheric pressure and T_{inlet} = 300 K.

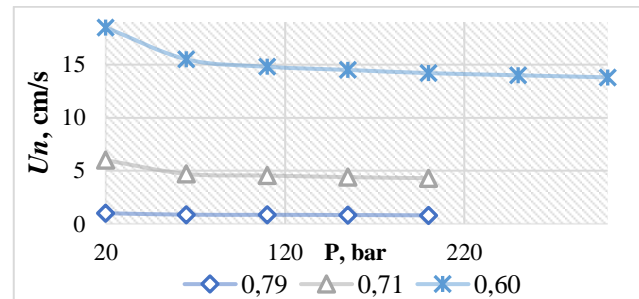


Figure-3. Flame propagation normal velocity vs pressure and diluter mass content γ (CO₂) at T_{inlet} = 300 K.

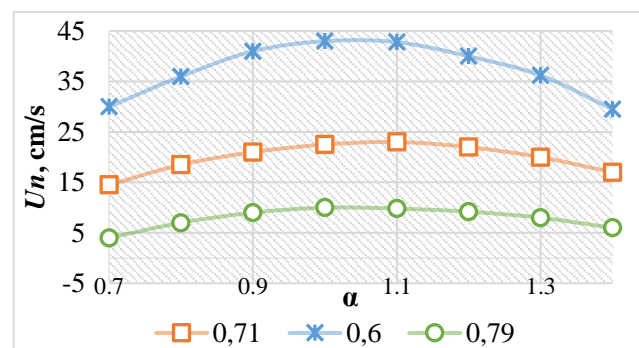


Figure-4. Flame propagation normal velocity vs CO₂ content in diluter at atmospheric pressure and T_{inlet} = 300 K.



It is worth mentioning that the detailed investigation of chemical aspect of combustion involves models of ideal mixing reactors. In actual combustors the ideal components mixing is hardly accessible so in the conditions of the gas motion assumptions which include the effective components mixing by large swirls and turbulence this approach results may be inadequate.

In this work is investigated the combined influence of pressure and diluent type not only in the

conditions of chemical kinetics limitations. The turbulent-kinetic interactions provide information on the flame structure and shape in the combustor space.

Investigation Object

The investigation object is the OFPF combustor shown in Figure-5.

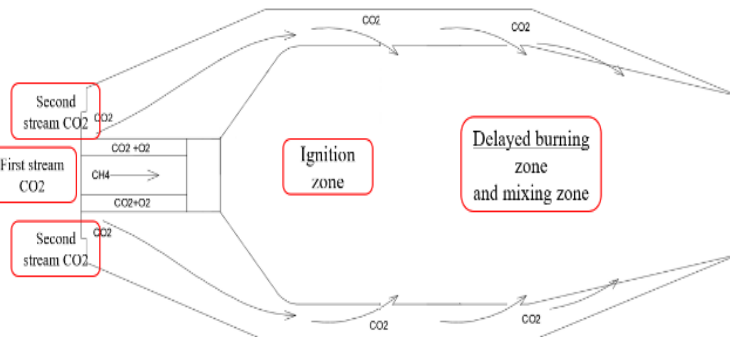


Figure-5. Flow chart of a combustor for oxy-fuel power production cycle with fluid flows distribution.

The considered cycle requires the carbon dioxide heating from 660 °C up to 1083 °C but the problem is to determine the fuel flow and the CO₂ diluent mass content in the OFPF combustor.

The fuel consumption may be calculated by the simple heat balance equation:

$$Q_{sh}^{CO_2} + Q_{sh}^{O_2} + Q_{cv.CH_4} = Q_{sh}^{(CO_2+CP)}$$

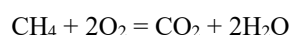
$Q_{sh}^{CO_2}$ - physical carbon dioxide heat at the combustor inlet, KWt;
 $Q_{sh}^{O_2}$ - physical oxygen heat, KWt;
 $Q_{sh}^{CH_4}$ - methane combustion value, KWt;
 $Q_{sh}^{CO_2+CP}$ - physical heat of CO₂ and products of methane combustion in oxygen.

Equation 2 determines the physical heat as the following:

$$Q = c_k \cdot t_k \cdot G_k$$

c_k - heat capacity at given pressure and temperature, KJ/kg°C;
 t_k - temperature, °C;
 G_k - massflow, kg/s.

The needed amount of methane may be determined through the products output from 1 kg methane combustion. The methane combustion with oxygen equation is the following:



Consideration of each component molar mass results with 1 kg methane requires 4 kg oxygen O₂ and produces 2.75 kg CO₂ and 2.25 kg H₂O. The required fuel consumption is 0.015 kg of CH₄ per 1 kg of CO₂. The calculated 560 kg of CO₂ requires 8.1 kg of CH₄ and 32.4 kg of O₂.

Most of gas turbines are equipped with a few combustors but the methane, oxygen and carbon dioxide mass ratios in each of the combustors is irrespective to the combustors number (Table-2).

Table-2. CH₄, O₂ and CO₂ supplied to combustor mass contents.

Component	Components mass ratio
CH ₄	0,013
O ₂	0,054
CO ₂	0,933

Mass diluent content in the OFPF combustor is 0.945 which is much higher than in standard gas turbines operating on air. Carbon dioxide and high pressure make an inhibiting effect so it is not reasonable to supply all CO₂ mixed with oxidizer. Part of it should be supplied to the active combustion zone as to reduce the flame tube metal maximal temperature.

Thus the carbon dioxide flow is split into two parts shown in picture-5:

- The first flow is supplied into the zone of methane and oxygen combustion.



- b) The second flow is supplied downstream the main combustion zone for convective cooling and the hot combustion products dilution.

The data on methane oxidizing [10] are a starting point for the combustor design concept:

- Not more than 20% of the total CO₂ flow may be supplied to the combustion zone. The main flow is supplied into the dilution zone, a larger supply into the combustion zone deeply reduces the flame propagation velocity,
- Not more than 10% of the CO₂ mixing flow, or the mass content γ below 0.634 is mixed with oxygen and supplied into the injector,
- The flame stabilization zone upstream the additional CO₂ supply must be at least 130 mm long.

The flame tube volume is determined out of the heat release intensity $Q_v = 700 \text{ KJ} / (\text{m}^3 \cdot \text{hr} \cdot \text{Pa})$ according to equation (4) [11]:

$$Q_v = \frac{3600 \cdot G_T \cdot Q_{cv} \cdot \eta}{V_k \cdot p_k} \quad (4)$$

G_T	- fuel massflow, kg/s;
Q_{cv}	- fuel heat productivity, KJ/kg;
η_f	- combustion efficiency;
V_k	- flame tube volume, m ³ ;
P_k	- Combustor exit pressure, Pa.

Recommended flame tube aspect ratio $L_k/H = 2,5$.

METHODS

The methane combustion with oxygen in supercritical pressure carbon dioxide environment is calculated in Ansys Fluent code. The turbulent-kinetic interaction analysis involved the Eddy Dissipation and Finite Rate Chemistry and the three-stage methane oxidation models. The components production and initial staff consumption velocities are determined by the following equations:

$$R = K(T) \cdot T^\beta \cdot (C_A) \cdot (C_B)$$

$$K(T) = A \cdot e^{\left(\frac{-E_a}{RT}\right)}$$

A	- pre-exponent multiplier;
E_a	- activation energy;
T^β	- temperature coefficient;
C_A, C_B	- initial components contents.

The calculation time was reduced by the initial problem split into two parts as the following:

- a) Components supply to the injector, mixing and pre-swirl. The simulation goal was tuning optimal oxygen supply nozzles for the uniform CO₂, mixing with needed content distribution.
- b) Combustion simulation with convective wall cooling with additional CO₂ supply. Here only the combustion zone was considered but not the dilution one.

Figure-6 illustrates the flame tube concept design that includes the gas mixture supply nozzle, combustor casing and the CO₂ injection holes along the walls. Assumption of the wall heat flux for the border condition simulates the convective wall cooling channel.

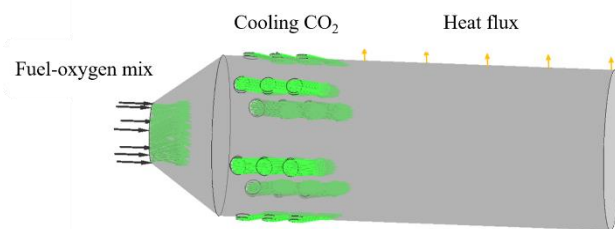


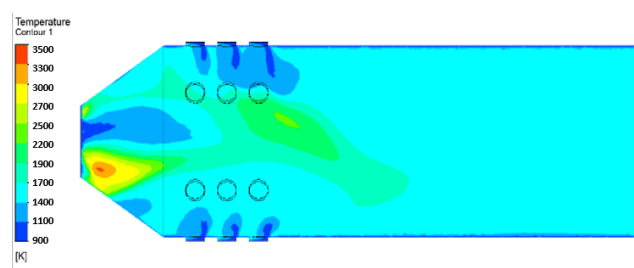
Figure-6. Combustor internal space design.

At the model inlet the fuel-oxidizer mixture massflow and contents distribution are taken from the injector simulation results. The holes inlet CO₂ flow is given in cylindrical coordinates that simulate the 60 ° nozzles inclination.

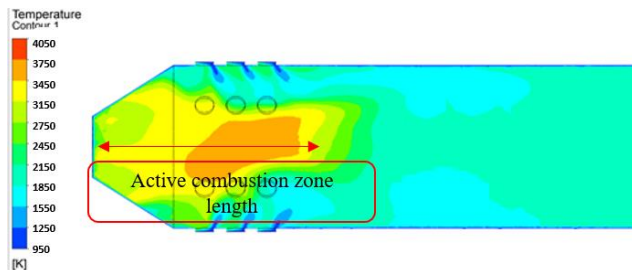
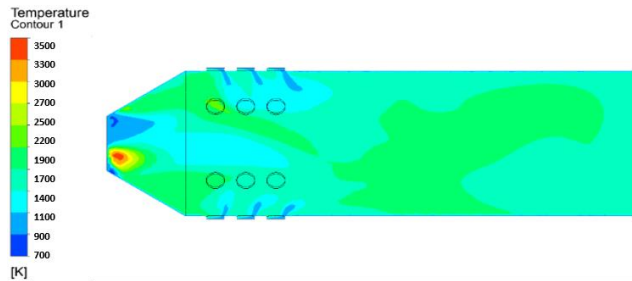
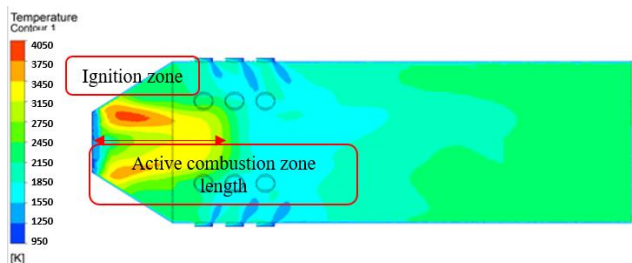
The simulation described two vane swirl angles of 30 and 45° and two diluent contents of 0.634 and 0.46.

CALCULATION RESULTS

The simulation results show that the CO₂ content of 0.634 in the active combustion zone suppresses the methane ignition and flame stabilization. The ignition is local and the flame is not anchored at the burner exit and when the flow enters the secondary CO₂ supply station the combustion process stops. This is shown by the chemical underburning values of 29 and 13% at the vane swirl angles 30 ° and 45 ° (Figure-7).



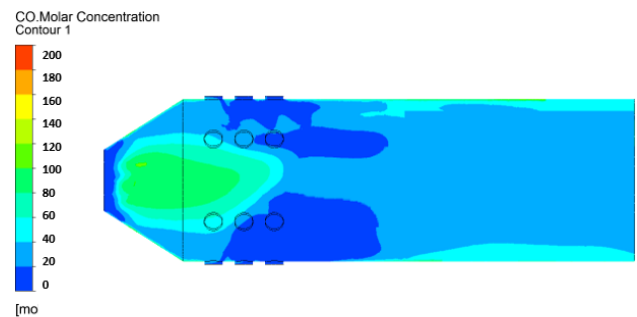
a) - vane swirl angle 30 °; $\gamma = 0,634$

b) - vane swirl angle 30° ; $\gamma = 0,460$ c) - vane swirl angle 45° ; $\gamma = 0,634$ d) - vane swirl angle 45° ; $\gamma = 0,460$ **Figure-7.** Temperature contours in the combustor cross-section.

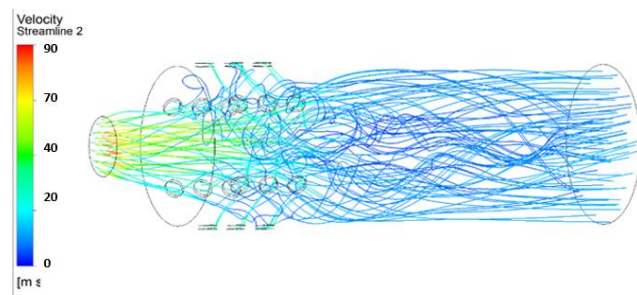
In the case $\gamma = 0,460$ and vane swirl angle 45° flame stabilizes at the burner exit and picture 7 r distinctly shows ignition zones. Length of the active combustion zone at swirl angle 30° it is 40% of the combustor length and at the angle 45° it shortens down to 20% of the combustor length and the active combustion is completed upstream the cooling CO_2 supply. The cone in the combustor inlet isolates the flame stabilization zone from the cooling CO_2 secondary flow.

In the area of CO_2 dilution steams penetrating the main flow its temperature drops down and the combustion process also slows down so the additional dilution CO_2 should be injected downstream the flame stabilization and main combustion zones.

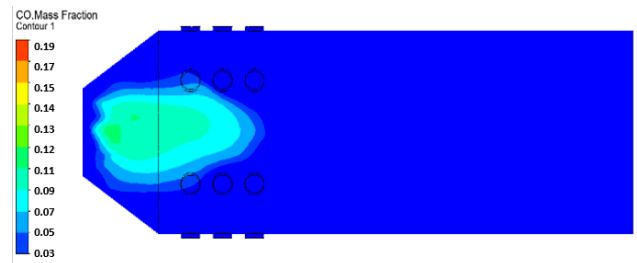
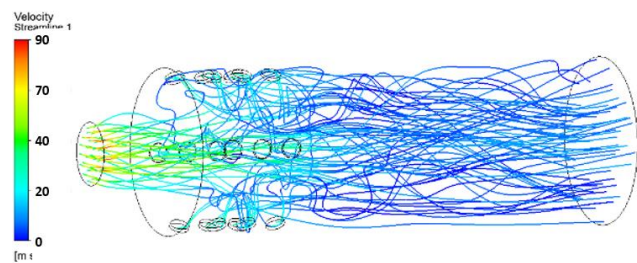
Figures 8 and 9 show the combustor carbon monoxide content and streamlines.



a) CO molar concentration in combustor transversal section



b) Flow streamlines

Picture-8. Simulation results at $\gamma_1 = 0,460$ and vane swirl angle 30° .a) vane swirl angle 45° ; $\gamma = 0,634$ b) vane swirl angle 45° ; $\gamma = 0,460$ **Figure-9.** Simulation results at $\gamma_1 = 0,460$ and vane swirl angle 45° .

Section subheadings should be typed bold-face, typed flush with the left-hand margin, and only the first letter of each major word is to be capitalised.



CONCLUSIONS

The CFD code computer simulation of the combustor flow structure, mixing and combustion allows the following conclusions:

- a) The combustor flame stabilization takes place at the content of CO₂ diluent supplied in a mixture with oxidizer below 0.46 - 0.5 and its further increase slows down combustion processes,
- b) Flow swirl stabilizes flame and reduces its length,
- c) Additional CO₂ diluent supply forms local low temperature zones which slows down the combustion process,
- d) The cooling CO₂ mixing into the flame stabilization zone should be eliminated,
- e) In the stable combustion conditions the combustor exit temperature and velocity distributions are uniform.

Based on these results the following may be recommended:

- The combustor carbon dioxide supply must be below 20% of its total flow. The supply should be split into two parts, mixed with oxidizer wt mass content below 0.5 and along the combustor walls for cooling. Thus the design may be based on traditional gas turbine combustors with some corrections.
- Flame stabilization and its length reduction require a swirl of the fuel-oxidizer- CO₂ mixture that may be provided by combustor inlet vanes,
- The velocity of fuel, oxidizer and CO₂ mixture supply into the combustor must be below 20 – 25 m/s, the cooling CO₂ supply velocity must be below 60% of that.
- The cooling CO₂ may enter at least 130 mm downstream the burner exit. The flame stabilization zone must be separated from the secondary cooling CO₂ flow.

ACKNOWLEDGMENTS

This study is conducted by Moscow Power Engineering Institute was financially supported by the Ministry of Science and Higher Education of the Russian Federation (project No. FSWF-2020-0020).

REFERENCES

- [1] Weizhong F. 2014. The research on design and technology of new high efficiency supercritical unit - a kind of cross-compound steam turbine generator unit in a manner of elevated and conventional layout. Proceedings of the 2nd IEA CCC Workshop on Advanced Ultras-Supercritical Coal-Fired Power Plants: 15-22.
- [2] Martin S., Forrest B., Rafati N., Lu X., Fetvedt J., McGroddy M. and Freed D. 2018. Progress update on the Allam cycle: commercialization of NET Power and the NET Power Demonstration Facility. Proceedings of the 14-th Greenhouse Gas Control Technologies Conference: 21-26.
- [3] Alenezi A. and Kapat J.S. 2019. Thermodynamic analysis of CO₂ Allam cycle for concentrated solar power complemented with oxy-combustion. Proceedings of AIAA Propulsion and Energy Forum: 4074.
- [4] Suzuki S., Iwai Y., Itoh M., Morisawa Y., Jain P., and Kobayashi Y. 2019. High pressure combustion test of gas turbine combustor for 50MWth supercritical CO₂ demonstration power plant on Allam cycle. Proceedings of the International Gas Turbine Congress.
- [5] Amato A.B., Hudak P.D., Carlo D., Noble D., Scarborough J., Seitzman T. and Lieuwen T. 2011. Methane oxy-combustion for low CO₂ cycles: Blowoff measurements and analysis. Journal of Engineering for Gas Turbines and Power. 133(6).
- [6] Polezhaev I.L. and Yu V. 2005. Normal flame propagation speed and analysis of the influence of system parameters on it. Thermophysics of high temperatures. 43: 933-942.
- [7] Karpov V.L., Mostinsky I.L., Polezhaev Yu.V. 2005. Laminar and turbulent regime of combustion of hydrogen flooded streams High Temperature Thermal Physics. 43(1): 115.
- [8] Lewis B., Elbe G. 1968. Combustion, flame and explosions in gases: trans. from English. p. 592.
- [9] Komarov I., Kharlamova D., Makhmutov B., Shabalova S. and Kaplanovich I. 2020. Natural Gas-Oxygen Combustion in a Super-Critical Carbon Dioxide Gas Turbine Combustor. E3S Web of Conferences. 178: 01027.
- [10] H. Wang, X. You, A.V. Joshi, S.G. Davis, A. Laskin, F. Egolfopoulos, C.K. Law. 2007. USC Mech Version II, High-temperature combustion reaction model of H₂/CO/C₁-C₄ compounds [Electronic resource]. Available at: http://ignis.usc.edu/Mechanisms/USCMech%20II/USC_Mech%20II.htm.
- [11] Rybalko V.V. 2002. Technique of thermal calculation of gas turbine power plants. p. 120.